Nucleotide Exchange and cGMP Phosphodiesterase Activation by Pertussis Toxin Inactivated Transducin†

Latha Ramdas, Rose M. Disher, and Theodore G. Wensel*
Department of Biochemistry, Baylor College of Medicine, Houston, Texas 77030
Received May 17, 1991; Revised Manuscript Received September 12, 1991

ABSTRACT: Transducin, the signal coupling protein of retinal rod photoreceptor cells, is one of a family of G proteins that can be inactivated by pertussis toxin. We have investigated the nature of this inactivation in order to determine (1) whether it requires the toxin-catalyzed transfer of ADP-ribose from NAD^+ to cysteine-347 of the α subunit and (2) whether it involves locking the α subunit in the inactive conformation characteristic of its GDP-bound state, or is limited to disruption of binding to photoexcited rhodopsin (R*). Our results indicate that all observed effects of pertussis toxin treatment, including a shift in the electrophoretic mobility of transducin's α subunit and functional inactivation, require NAD^+ and that the appearance of the shift parallels incorporation of ADP-ribose. We have also found that, apart from interactions with photoexcited rhodopsin, the functional properties of ADP-ribosylated transducin are essentially the same as those of unmodified transducin. Normal spontaneous nucleotide exchange kinetics and the ability to activate cGMP phosphodiesterase are preserved following quantitative ADP-ribosylation, as are the abilities to hydrolyze GTP, to bind to a dye affinity column, and to display enhanced fluorescence upon addition of Al^{3+} and F^-. Thus, ADP-ribosylation merely blocks catalysis of transducin nucleotide exchange by R* and does not lock transducin in an inactive state. Analysis of spontaneous nucleotide exchange kinetics required following nucleotide uptake for many hours, and revealed that over the range 10–100 μM GTPγS, exchange of GDP for GTPγS occurs with an apparent first-order rate constant of (0.9–2) $\times 10^{-4}$ s^{-1}, when either GTPγS binding or GDP release is monitored. This exchange rate is slower than those that have been reported for other G proteins and implies that the enhancement of the nucleotide exchange rate by photoexcited rhodopsin is on the order of 10^7-fold.

One of the early indications of the striking structural and functional homology between transducin (T),[1] the G protein of retinal rod outer segments (ROS), and the G proteins coupled to hormone receptors [reviewed by Stryer and Bourne (1986), Gilman (1987), and Birnbaumer (1990)] was the finding that pertussis toxin (PTX) catalyzes ADP-ribosylation of the α subunit of transducin (Van Dop et al., 1984) as well as those of G_i (Katada & Ui, 1982; Codina et al., 1983; Bokoch et al., 1983) and G_o (Sternweis & Robishaw, 1984). The ADP-ribosylation site is Cys-347, four amino acid residues from the carboxyl terminus (West et al., 1985).

ADP-Ribosylation of transducin by PTX has been shown to abolish light-stimulated hydrolysis of GTP and cGMP in ROS from bovine retina (Van Dop et al., 1984; Watkins et al., 1984), and the preferred substrate for ADP-ribosylation was reported to be the inactive GDP binding conformation. Thus, pertussis toxin appeared to "lock" transducin in the GDP (inactive) site. One clear symptom of this inactive state (Van Dop et al., 1984) is the disruption by PTX of transducin's interaction with photoexcited rhodopsin (R*). However, it has not been determined whether ADP-ribosylated transducin is capable of undergoing nucleotide exchange in the same way as unmodified protein, or of undergoing the GTP-triggered conformational shift characterized by dissociation of T_α from $T_{\beta\gamma}$, by activation of cGMP phosphodiesterase (PDE) (Fung et al., 1981), and by enhanced tryptophan fluorescence (Phillips & Cerione, 1988). It has been reported (Rybin et al., 1989) that pertussis toxin treatment eliminates the ability of purified transducin to release bound GDP slowly in the absence of R*, to hydrolyze GTP, and to activate PDE, consistent with direct effects of ADP-ribosylation on transducin's nucleotide binding properties and on T_α's ability to assume the active conformation.

In some systems, GTP or nonhydrolyzable analogues appear to exert certain functional effects presumed to be mediated by G proteins after PTX treatment (Hildebrandt et al., 1983; Masters et al., 1985; Huff & Neer, 1986; Sunyer et al., 1989), suggesting that G-protein–effector interactions may not be blocked by ADP-ribosylation. Studies in cells or crude membranes may be complicated, however, by the presence of pertussis toxin insensitive GTP binding proteins (Fong et al., 1988; Strathmann & Simon, 1990) in addition to the pertussis toxin sensitive G proteins. Reconstitution of full effector-stimulating activity with purified G proteins quantitatively ADP-ribosylated by pertussis toxin has been difficult to demonstrate. Determination of the ability of ADP-ribosylated transducin to activate PDE has been hampered by the difficulty of loading an activating nucleotide (e.g., GTPγS) into the α subunit in the absence of R*-catalyzed nucleotide exchange.

New questions about the effects of pertussis toxin have been raised by a report that in brain membranes, $G_{i\alpha}$ subunits are modified by pertussis toxin in a reaction that does not involve NAD^+ or ADP-ribosylation (Ribeiro-Neto & Rodbell, 1989).

† This work was supported by National Institutes of Health Grants EY07981 and RR05425 and by the Robert A. Welch Foundation.

[1] Abbreviations: T, transducin, the photoreceptor G protein; T_α and $T_{\beta\gamma}$, α and $\beta\gamma$ subunits of transducin; ROS, rod outer segment(s); PDE, photoreceptor cGMP phosphodiesterase; PTX, pertussis toxin; R*, photoexcited rhodopsin (metarhodopsin II); SDS, sodium dodecyl sulfate; MOPS, 4-morpholinepropanesulfonic acid; DTT, dithiothreitol; Tris, tris(hydroxymethyl)aminomethane; GppNHp, guanyl-5′-yl imidodiphosphate; GTPγS, guanosine 5′-*O*-(3-thiotriphosphate).

0006-2960/91/0430-11637$02.50/0

The chief indications of this modification are an altered electrophoretic mobility in gels and a change in immunoreactivity that had previously been attributed to ADP-ribosylation.

There has also been some uncertainty concerning the kinetics of guanine nucleotide exchange by transducin in the absence of R*. Other heterotrimeric G proteins bind nucleotides spontaneously with second-order rate constants in the range 10^6–10^7 M^{-1} s^{-1} in the absence of bound GDP (Ferguson et al., 1986), but display essentially first-order kinetics at GTP or GTPγS concentrations from 10 nM to 100 μM in the normal GDP-bound state (Northup et al., 1982). These results have been interpreted as limited by the rate of GDP release, which is governed by first-order rate constants in the range 4.7×10^{-4} to 6×10^{-3} s^{-1} (Ferguson et al., 1986; Northup et al., 1982). In contrast, it has been reported (Wessling-Resnick & Johnson, 1987) that GTPγS binding to GDP–transducin occurs with second-order kinetics up to 10^{-6} M GTPγS and that the rate constant for the exchange reaction is 2×10^7 M^{-1} s^{-1}. It has been reported (Fawzi & Northup, 1990) that occasional observation of rapid nucleotide exchange by transducin (i.e., on a time scale of minutes) can be attributed to contamination with traces of R*. In previous studies, the time course of transducin nucleotide exchange in the absence of R* has not been followed for sufficient time to ensure that equilibrium was reached. On the basis of the results described below, at 37 °C an incubation time between 6 and 13 h is required before the reaction is within 1% of equilibrium. Even longer times are needed at the lower temperatures (23–30 °C) employed in most previous studies.

In order to address these uncertainties, we have carried out experiments designed to answer the following questions about transducin: (1) Is NAD^+ required for the electrophoretic mobility shift and functional inactivation induced by pertussis toxin? (2) What are the kinetics of nucleotide exchange in the absence of R* when followed for many hours? (3) Is the inhibition of nucleotide exchange by pertussis toxin treatment simply a consequence of a disruption of R* binding, or are there direct effects on the nucleotide binding site? (4) Is PTX blockage of transducin's ability to stimulate cGMP phosphodiesterase (PDE) simply an indirect consequence of loss of rapid nucleotide exchange, or is pertussis toxin inactivated transducin incapable of undergoing the normal GTP-triggered conformational change to its activated state?

Materials and Methods

Reagents. GTPγS, ATP, GDP, MOPS, and DTT were obtained from Boehringer-Mannheim. EDTA was from Fisher Scientific. [^{35}S]GTPγS and [*adenylate*-^{32}P]NAD^+ were from New England Nuclear. [^{3}H]cGMP was from ICN. Reagents for electrophoresis were from Bio-Rad. Pertussis toxin was from List Biological Laboratories (Campbell, CA). Frozen dark-dissected bovine retinas were obtained from J. A. Lawson Packing (Lincoln, NE). Other reagents were obtained from Sigma Chemical Co.

Buffers. ROS buffer contained 10 mM MOPS, pH 7.5, 30 mM NaCl, 60 mM KCl, 2 mM $MgCl_2$, 1 mM DTT, and 0.1 mM phenylmethanesulfonyl fluoride (PMSF). Pertussis toxin activation and ADP-ribosylation buffer contained 20 mM Tris-HCl, pH 7.6, 2 mM EDTA, 20 mM DTT, and 1 mM ATP. Radioactivity assay buffer contained 0.1 M Tris-HCl, pH 8.0, 2 mM $MgCl_2$, 50 mM KCl, and 1 mM DTT. The pH assay buffer contained 20 mM MOPS, pH 8.0, 150 mM KCl, and 2 mM $MgCl_2$. HPLC gel filtration buffer contained 0.1 M Tris-HCl, pH 7.5, 3 mM $MgCl_2$, 1 mM EDTA, 60 mM KCl, 30 mM NaCl, and 1 mM DTT. Subunit separation buffer contained 10 mM Tris-HCl, pH 8.0, 5 mM $MgCl_2$, 0.1 mM EDTA, and 1 mM DTT.

Rod Outer Segments and Protein Preparation. Rod outer segments (ROS) were prepared under dim red light from frozen dark-dissected bovine retinas as described (Fung & Stryer, 1980). Transducin was prepared by GTP elution of hypotonically washed ROS and chromatography on hexyl-agarose as described (Fung et al., 1981). Transducin used for activation of PDE was further purified by HPLC gel filtration using a Superose 12 column (Pharmacia) to remove traces of contaminating PDE. PDE (Wensel & Stryer, 1990) and urea-stripped ROS membranes devoid of peripheral proteins (Yamanaka et al., 1985) were prepared as previously described. Solutions of purified proteins were made 50% (v/v) in glycerol and stored at −20 °C.

Cibacron Blue Affinity Chromatography. Purified transducin (60 μg) was treated with pertussis toxin and [^{32}P]NAD^+ as described below and then loaded onto a 1-mL column of Reactive Blue Sepharose CL-6B (Sigma) equilibrated with subunit separation buffer. The column was washed with this buffer containing 100 mM NaCl, and the bound T_α was eluted with the same buffer containing 750 mM NaCl and 100 μM GTP. Fractions (1 mL) were collected and analyzed by SDS–polyacrylamide gel electrophoresis and autoradiography.

Electrophoresis. SDS–polyacrylamide gel electrophoresis was carried out essentially according to the method of Laemmli (1970) except that the concentration of acrylamide varied in a linear gradient from 12% to 20% (w/v), and proteins were precipitated with 5% (w/v) trichloroacetic acid before being dissolved in sample application buffer. Protein bands were visualized with Coomassie blue stain.

ADP-Ribosylation with Pertussis Toxin. Pertussis toxin (500 μg/mL) was activated in the PTX activating buffer for 30 min at 30 °C. In some cases, 1% (w/v) Lubrol-PX was included in the activation mixture in order to approximate the reaction conditions used for G_i (Ribeiro-Neto & Rodbell, 1989); however, no differences were observed between PTX effects obtained with Lubrol-PX and those obtained without the detergent. Transducin was treated with activated pertussis toxin (20 μg/mL) and 2 mM NAD^+ unless otherwise specified. When [^{32}P]NAD^+ was used, it was at a specific activity of 13–100 mCi/mmol. The reaction mixture and the control (lacking NAD^+, but otherwise identical) were incubated for 30 min at 30 °C. For ADP-ribosylation of ROS membranes, the membranes were incubated in the dark with the same reaction components as for the purified protein, plus 200 μM GDP. The reaction was allowed to continue for 2 h at 30 °C or overnight at 4 °C. ADP-Ribosylation of transducin in the membranes was determined either by monitoring incorporation of radioactivity into T_α (using SDS–polyacrylamide gel electrophoresis followed by autoradiography and scintillation counting of excised T_α bands) or by monitoring the loss of GTPγS- and light-dependent PDE stimulation. ADP-Ribosylation of purified transducin was monitored either by using [^{32}P]NAD^+ or by observing the shift in the electrophoretic mobility of T_α as compared to native T_α in SDS–polyacrylamide gels. Using the conditions described above and [^{32}P]NAD^+, it was found that 1.01 (±1.09) mol of ADP-ribose was incorporated per mole of transducin (average of three separate preparations). Prolonged incubation (up to 24 h) at 37 °C resulted in no detectable loss of the ADP-ribosyl moiety, as determined by autoradiography and scintillation counting of gels loaded with [^{32}P]ADP-ribosylated transducin. Because most of our assays for transducin activity used radioisotopes, and because of uncertainties introduced by degradation of

stocks of [^{32}P]NAD$^+$ upon storage (Latha Ramdas and James B. DeMar, unpublished results) and by possible inaccuracies in the dye binding protein assays, the mobility shift assay was routinely used to verify quantitative ADP-ribosylation of all transducin samples used for functional assays. For the nucleotide exchange and hydrolysis experiments described below, it was also verified in each case that the ADP-ribosylated transducin used had less than 10% of the rapid R*-dependent nucleotide exchange and hydrolysis activity of the control sample treated without NAD$^+$.

In general, PTX and NAD$^+$ were not removed after the labeling procedure. NAD$^+$ by itself did not affect the activity of transducin in any of the assays described here. PTX by itself or with NAD$^+$ did not display any activity in these assays.

Nucleotide Exchange and Hydrolysis Kinetics. Nucleotide uptake was monitored by nitrocellulose filter binding as described (Yamanaka et al., 1985). Reactant concentrations unless otherwise indicated were 2 μM transducin and 10 μM [^{35}S]GTPγS (3–5 Ci/mmol) in ROS buffer. Nonspecific binding was determined from measurements in which excess cold GTPγS was added before radioactive nucleotide, and was less than 0.5% of the maximum specific binding. The kinetics of GDP dissociation were monitored using ADP-ribosylated or native transducin (2 μM) that had been incubated for 20 h with [α-^{32}P]GTP (10 μM) at 23 °C. GTPγS was then allowed to exchange for the bound [α-^{32}P]GDP ([α-^{32}P]GTP is hydrolyzed to [α-^{32}P]GDP; Fung & Stryer 1980) and any remaining bound [α-^{32}P]GTP. The reaction was initiated by addition of 100 μM GTPγS to the reaction mixture at 37 °C, and the release of radiolabeled GDP was monitored at specified times by filter binding. For GTP hydrolysis measurements, transducin (2 μM) was incubated with 10 μM [α-^{32}P]GTP in ROS buffer containing 1.0 mM ATP (to inhibit traces of nonspecific nucleotidase activity) at 37 °C. The progress of the reaction was followed by removing aliquots of the reaction mixture and quenching with trifluoroacetic acid on ice at specified times. The samples were analyzed by poly(ethylenimine)–cellulose thin-layer chromatography using 750 mM KH_2PO_4, pH 3.7. Radioactive nucleotides were visualized by autoradiography, the spots were cut out, and ^{32}P was quantitated by scintillation counting. Stoichiometry for all radiolabeled nucleotides was determined from the specific activity and radioactivity measured by scintillation counting of nitrocellulose filters or of material scraped from TLC plates.

Other Assays. PDE activity was measured as described (Wensel & Stryer, 1986) using either a single time point assay with [^{3}H]cGMP (Thompson & Appleman, 1971; Hurley & Stryer, 1982) or a continuous pH assay (Liebman & Evanczuk, 1982). Protein concentration was determined by the Coomassie blue binding method (Bradford, 1976). Intrinsic fluorescence of transducin was measured using an Aminco–Bowman spectrofluorometer (J4-8960) modified in the following ways: The detector was replaced with an R928 photomultiplier connected to a Keithley 527 current amplifier, whose signal was transferred to a personal computer through a DAS 16G (Metrabyte) analogue-to-digital convertor. A 280-nm interference filter was used in the excitation path, and a 305-nm cuton (50% transmittance) high-pass filter was used in the emission path to improve stray light rejection. The protein was excited at 280 nm and the emission spectrum recorded between 285 and 385 nm. The observed emission maximum was 336 nm. Transducin solutions containing NAD$^+$ were diluted to obtain an absorbance less than or equal to 0.03 at 280 nm to minimize inner filter effects. At these concentrations, neither NAD$^+$ nor PTX contributed significantly to the observed fluorescence and, besides inner filter effects, did not significantly affect transducin's fluorescence.

All results reported were repeated at least 3 times, and points plotted with error bars in the figures represent the mean ± the standard deviation for triplicate samples in representative experiments. Fits to theoretical curves were obtained by computerized nonlinear least-squares analysis.

Results

NAD$^+$ Is Required for a PTX-Induced Shift in Electrophoretic Mobility. Under conditions very similar to those used to demonstrate NAD$^+$-independent modification of $G_{i\alpha}$ in brain membranes (Ribeiro-Neto & Rodbell, 1989), purified transducin was treated with pertussis toxin in the presence or absence of 2 mM NAD$^+$. As shown in Figure 1, PTX induces a decline in T_α's electrophoretic mobility when NAD$^+$ is included but has no effect on its mobility in the absence of NAD$^+$. The two forms can be clearly resolved, as can be seen in the gel lanes in which transducin treated with PTX and NAD$^+$ was mixed with transducin treated with PTX and no NAD$^+$ before being loaded on the gel. Comparison of the autoradiogram with the mobility shifts (Figure 1, bottom) observed over a range of NAD$^+$ concentrations reveals a strong correlation between incorporation of ^{32}P (presumably as ADP-ribose) and the mobility shift. Thus, the mobility shift serves as a simple assay for ADP-ribosylation of transducin.

NAD$^+$ Is Required for Functional Inactivation by PTX. PTX inactivation was assayed using three different transducin activities: R*-catalyzed nucleotide exchange, R*-stimulated GTP hydrolysis, and GTP-dependent PDE activation. In each case, the sample treated with NAD$^+$ showed inactivation, while very little effect was observed when NAD$^+$ was omitted. As shown in the inset to Figure 2A, purified transducin treated with PTX in the presence of NAD$^+$ shows very slow uptake of GTPγS in the presence of R*, whereas transducin treated with PTX but without NAD$^+$ undergoes the rapid R*-catalyzed nucleotide exchange that is characteristic of the unmodified protein. Similar results were obtained for R*-stimulated GTPase activity (Figure 3 inset). Likewise, illuminated ROS membranes that had been treated with PTX in the presence of NAD$^+$ showed no activation of cGMP phosphodiesterase when GTP was added (Figure 4A). In contrast, ROS treated with PTX in the absence of NAD$^+$ showed normal stimulation of PDE by GTP. This requirement for NAD$^+$ in order for PTX to inactivate transducin was also observed by Rybin et al. (1989).

Nucleotide Exchange by Unmodified Transducin in the Absence of R.* In order to determine the effects of ADP-ribosylation on spontaneous nucleotide exchange, it was necessary first to characterize the nucleotide binding properties of the native protein in the absence of R*, by carrying out exchange experiments over periods of many hours. Figure 2B shows the results for unmodified transducin obtained at 10 and 30 μM GTPγS. A reasonable fit is obtained for the uptake if the kinetics are modeled as first order, with a rate constant of 1.17×10^{-4} s^{-1}. When R* was added to transducin after an overnight incubation, no additional binding was observed (data not shown), indicating that the nucleotide binding site occupied during R* catalyzed exchange was involved in the spontaneous exchange reaction. The kinetics are complicated somewhat by the existence of one or more low-affinity binding sites (Bennett & Dupont, 1985; Sitaramayya et al., 1988) in addition to the high-affinity site that dominates the kinetics at 10 μM GTPγS. Our equilibrium binding results (Figure 2B inset) are consistent with the existence of heterogeneous binding sites: a poor fit is obtained using a single high-affinity

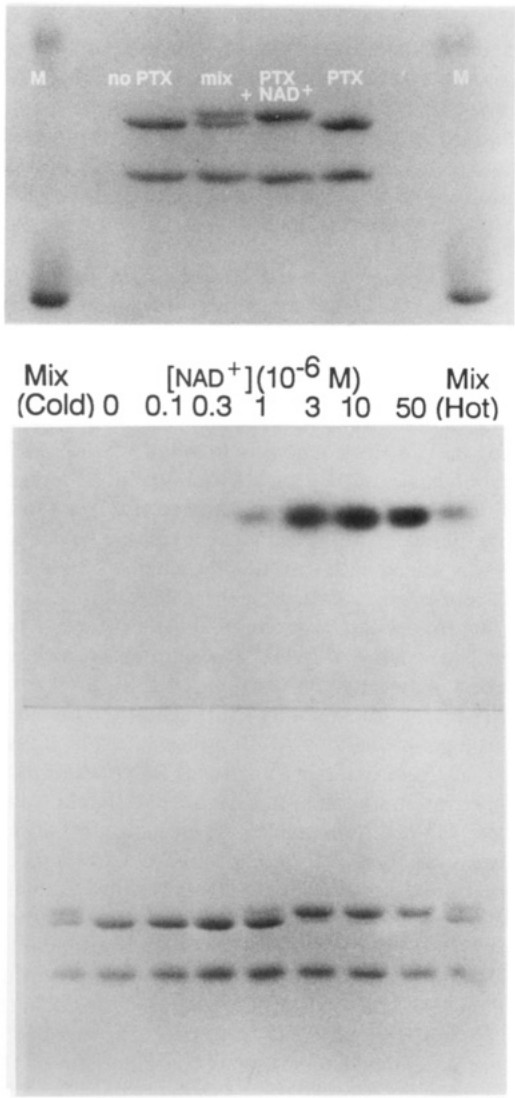

FIGURE 1: NAD^+ dependence of pertussis toxin induced shift in electrophoretic mobility. (Top panel) Coomassie blue stained gel. From left to right: M, molecular mass markers (ovalbumin, 45 kDa; carbonic anhydrase, 30 kDa); no PTX, untreated transducin; mix, a 50:50 mixture of the PTX reaction mixtures with and without NAD^+; PTX + NAD^+, transducin treated with PTX and NAD^+; PTX, transducin treated with PTX in the absence of NAD^+. (Bottom panel) Bottom section: Coomassie blue stained gel. The uppermost bands are ADP-ribosylated (higher) and unmodified (lower) T_α. The lowest dye-stained band in each transducin lane is the β subunit, whose mobility is unaffected by PTX. Upper section: autoradiogram of same gel. The first lane, labeled "Mix (Cold)", contained an equimolar mixture of ADP-ribosylated (nonradioactive) and non-ADP-ribosylated transducin. The other lanes contained transducin treated with PTX and the indicated concentrations of [^{32}P]NAD^+, except for the last lane, labeled "Mix (Hot)", which contained samples from the 0 NAD^+ and 50 μM NAD^+ reactions, mixed in equal proportions after TCA precipitation and SDS solubilization. Each lane contained approximately 1.4 μg of transducin.

binding site model (Figure 2B inset, dashed line) even if K_d is assumed to be 1 μM, a value much higher than the previously reported values of 50–70 nM (Yamanaka et al., 1985; Kelleher et al., 1986) for the high-affinity site. However, good fits are obtained using models with two or three binding sites with different K_d values; for example, if it is assumed that K_d for the high-affinity sites is 100 nM, then a good fit is obtained if 70% of the total sites are low affinity with K_d = 45 μM (Figure 2B inset, solid curve). As the nucleotide concentrations examined do not extend beyond this higher K_d value, or below the lower one, we do not attribute quantitative significance to this fit, but it provides an order of magnitude estimate for the low-affinity site(s). We have not characterized the low-affinity site(s) in any further detail, but we have obtained biphasic binding curves with both [α-^{32}P]GTP and [^{35}S]-GTPγS.

ADP-Ribosylation Does Not Block Spontaneous Nucleotide Exchange. The nucleotide exchange results displayed in the inset to Figure 2A do not distinguish between a disruption of R* binding, which is known to occur (Van Dop et al., 1984), and direct effects on transducin's nucleotide binding properties. This distinction can be made by observing nucleotide exchange in the absence of R*. A comparison of the kinetics of GTPγS binding to transducin in the absence of R* (Figure 2A), following PTX treatment with and without NAD^+, indicates very little change upon ADP-ribosylation. In some experiments, ADP-ribosylated transducin bound slightly more GTPγS or GDP at equilibrium, and in others, it bound slightly less than native transducin. The differences between the two forms were in general less than 20% of the total bound nucleotide. Because the rate appears to be limited under these conditions by GDP release, this experiment does not rule out some differences in affinity for GTPγS, but argues against dramatic changes in the affinity for GTPγS. The somewhat decreased stoichiometry of binding displayed by PTX-treated transducin (0.33 GTPγS per transducin with or without NAD^+, Figure 2A) as compared to untreated transducin (0.55 GTPγS per transducin, Figure 2B) is probably due to thermal inactivation of transducin during prolonged incubations at 30 °C and 37 °C rather than to a specific action of PTX because (1) it does not depend on NAD^+ (Figure 2A) and (2) it was not observed during rapid R*-catalyzed exchange (Figure 2A inset, 0.57 GTPγS per transducin).

When GDP release was measured in the presence of an excess of GTPγS (100 μM), the release rates for ADP-ribosylated and native transducin were found to be similar (Figure 2C). The best-fit k_{off} for the ADP-ribosylated transducin was 1.97×10^{-4} s^{-1}, and for the control, it was 1.4×10^{-4} s^{-1}. The inset to Figure 2C shows that the nucleotide exchange rate constants for GTPγS concentrations from 10 to 100 μM fall in the range of $(0.9–2) \times 10^{-4}$ s^{-1} whether transducin is ADP-ribosylated or not, and whether GTPγS binding or GDP release is monitored. The weak dependence of the rate constant on [GTPγS] is consistent with the kinetics being dominated by the first-order process of GDP release, but with small effects apparent at high [GTPγS] possibly reflecting the low-affinity binding sites.

ADP-Ribosylation Does Not Block GTP Hydrolysis. In addition to binding GTP, native transducin also catalyzes its hydrolysis, an essential step in the deactivation of the cGMP cascade. A comparison of the rates of GTP hydrolysis catalyzed by equal concentrations of transducin that had been PTX-treated with and without NAD^+ (Figure 3) shows no inhibition of GTPase activity due to ADP-ribosylation. Because the hydrolysis rate is presumably limited by the rate of GDP release, this experiment does not actually indicate whether the rate constant for hydrolysis of bound GTP changed, but it does indicate that ADP-ribosylated transducin, like native transducin, hydrolyzes GTP faster than it releases bound GDP. The turnover number observed ($\sim 0.1 \times 10^{-4}$ s^{-1}) with both ADP-ribosylated and non-ADP-ribosylated transducin is about one-third of what would be expected from the GDP release rate and the fraction of treated transducin that binds nucleotide. The activity may be low due to inhibition by the 1 mM ATP that was present or by unlabeled GTP contaminating the ATP, or due to some transducin that binds but does not hydrolyze GTP, as has been suggested may be

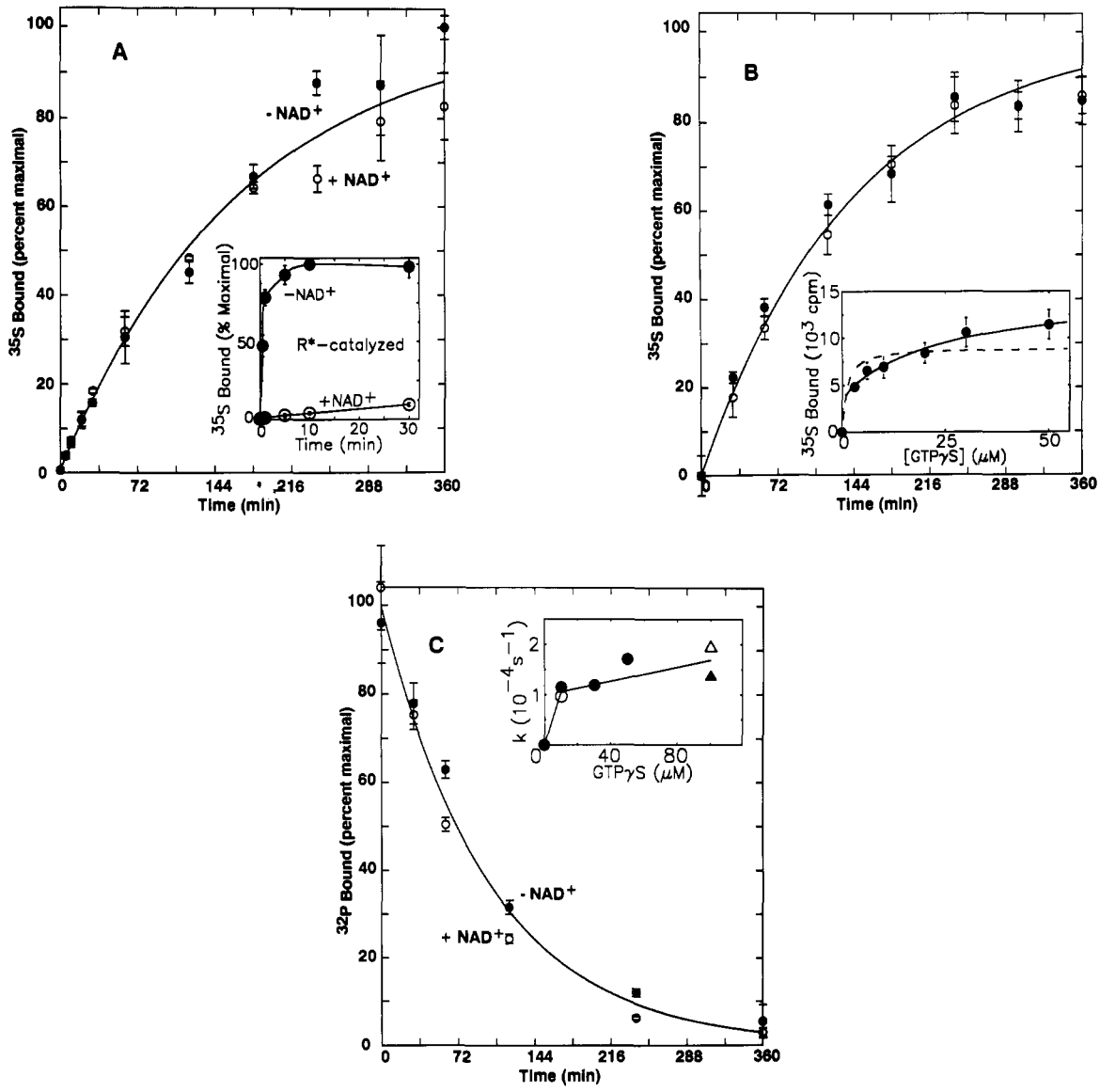

FIGURE 2: Nucleotide exchange kinetics. (A) Transducin treated with PTX in the presence or absence of NAD^+. Uptake of [^{35}S]GTPγS (10 μM, 4.3 Ci/mmol) by transducin (2 μM) was monitored at 37 °C by filtration of 10-μL aliquots. The curve was calculated using $B = B_{max}[1 - \exp(-kt)]$ where B = bound radioactivity, t = time, and the values of B_{max} (62 250 cpm) and k (9.7×10^{-5} s^{-1}) were obtained by nonlinear least-squares fitting. Results are plotted as percent of B_{max}. The actual maximal binding after 24 h was 60 000 cpm (+NAD^+) or 62 000 cpm (-NAD^+). Inset: Conditions were identical, except that 0.5 μM R* (urea-stripped ROS membranes) was added. Note time scale difference. The maximal binding for the -NAD^+ sample (100%) was 107 000 cpm. (B) Untreated transducin. Transducin (2 μM) was incubated for the indicated time with [^{35}S]GTPγS (3.5 Ci/mmol) before filtration. Open circles, 10 μM GTPγS; closed circles, 30 μM GTPγS. The theoretical curve was calculated as in (A) using $k = 1.17 \times 10^{-4}$ s^{-1}. Results are plotted as percent of the maximum binding observed after 24 h: B_{max} = 80 430 cpm (10 μM GTPγS) and B_{max} = 115 700 cpm (30 μM GTPγS). Inset: GTPγS bound to transducin (0.2 μM) following a 22-h incubation at 37 °C with the indicated concentrations of GTPγS. Dashed line: curve obtained from least-squares fit for number of sites, assuming a single class of high-affinity binding sites with K_d = 1 μM. Solid line: best-fit curve for two classes of sites, with an assumed K_d of 0.1 μM for the high-affinity sites and K_d = 45 μM (derived from the fit) for the low-affinity sites. (C) GDP release by native and ADP-ribosylated transducin. Transducin (2 μM) was allowed to bind [α-^{32}P]GDP by incubation with [α-^{32}P]GTP (10 μM, 0.86 Ci/mmol) as described in the text. Aliquots (20 μL) were removed and filtered just before (t = 0) and at various times after addition of 100 μM GTPγS. The curve was calculated according to $B = B_{max} \exp(-kt)$ where $k = 1.64 \times 10^{-4}$ s^{-1} (from simultaneous least-squares fit of data from both conditions) and B_{max}(100%) = 15 100 cpm (mean of six samples). Results are plotted as percent of B_{max}. Inset: Nucleotide exchange rate constants as a function of [GTPγS]. Open circle, GTPγS uptake, PTX treated with or without NAD^+; closed circles, GTPγS uptake, untreated transducin; open triangle, GDP release, PTX treated with NAD^+; closed triangle, GDP release, PTX treated without NAD^+.

formed during purification (Sitaramayya et al., 1988). The early burst of activity may be due to some transducin that did not have GDP bound initially.

Enhancement of Tryptophan Fluorescence in ADP-Ribosylated Transducin. Native transducin not only binds GTP and its analogues but also undergoes a conformational change that reduces the affinity of T_α for $T_{\beta\gamma}$, and confers on T_α the ability to activate PDE. One direct physical indicator of this conformational change is an enhancement of the intrinsic tryptophan fluorescence of transducin which accompanies activation by GTP, GTPγS, or AlF_4^- (Phillips & Cerione, 1988). Aluminum and fluoride have been reported to inhibit GTPase activity by promoting $T_{\beta\gamma}$ dissociation from T_α (Kanaho et al., 1985). When the fluorescence enhancement upon addition of 5 mM NaF (along with 20 μM $AlCl_3$ and 10 mM $MgCl_2$) to transducin–PTX treated with NAD^+ was compared to that observed for an identical sample treated with the labeling buffer but without NAD^+ or PTX, no difference was observed (data not shown). Both samples showed a lower level of fluorescence enhancement (10%) than did untreated transducin (36%). These results suggest that activating ligands trigger a conformational change in ADP-ribosylated transducin

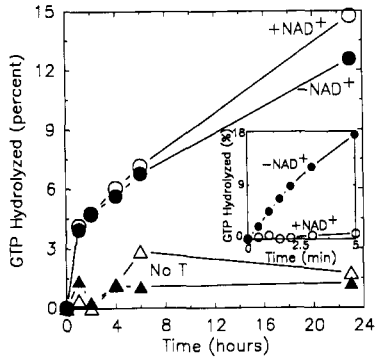

FIGURE 3: GTPase activity of native and ADP-ribosylated transducin. Circles: purified transducin was treated with PTX in the presence (open) or absence (closed) of NAD^+, and GTP hydrolysis was assayed as described in the text using 2 μM transducin and 10 μM [α-^{32}P]GTP (1 Ci/mmol). The percentage of total GTP hydrolyzed is plotted. Triangles: samples without transducin that otherwise were treated identically, with (open) or without (closed) NAD^+. Inset: GTP hydrolysis in the presence of 0.1 μM R*. Note the time scale difference.

similar to the one they trigger in native transducin, and also provide additional evidence for selective (but ADP-ribosylation-independent) loss of certain transducin functions upon prolonged incubation.

Cibacron Blue Affinity Column Binding. Immobilized Cibacron blue can be used to separate transducin subunits (Shinozawa et al., 1980; Watkins et al., 1985) because the α subunit binds to the dye and releases $\beta\gamma$. T_α is then eluted by high salt. When this procedure was applied to ADP-ribosylated transducin, the elution profiles of the $\beta\gamma$ and α subunits were indistinguishable from those obtained with untreated transducin (data not shown), indicating that the site(s) for interaction with the dye column had not been blocked by ADP-ribosylation.

ADP-Ribosylation Does Not Block Stimulation of cGMP Phosphodiesterase in ROS. As illustrated in Figure 4A, ADP-ribosylation blocks normal PDE activation by transducin. To determine whether this is a direct effect on T_α's sites of interaction with PDE or is simply due to slow nucleotide exchange kinetics, the first two steps in transducin activation, R* binding and nucleotide exchange, were shunted by addition of aluminum and fluoride ions to form aluminum tetrafluoride, which can directly activate native transducin in the GDP form (Bigay et al., 1985, 1987). As shown in Figure 4B, this treatment does stimulate PDE in ROS membranes, even after ADP-ribosylation of transducin, suggesting that the sites for interaction with PDE and those involved in the conformational changes accompanying the GDP to GTP transition are not inactivated by pertussis toxin.

ADP-Ribosylated Transducin Stimulates Purified cGMP Phosphodiesterase in Reconstituted Membranes. Using the spontaneous nucleotide exchange procedure described above, a nonhydrolyzable activator such as GTPγS can be incorporated into ADP-ribosylated transducin to determine whether it can activate PDE in this form as well. The modified protein was incubated with GTPγS for 6 h at 37 °C, and its PDE activation potency was compared with that of a control treated identically but without NAD^+. Figure 5 shows the results, measured using the [^{3}H]cGMP assay and membranes reconstituted from urea-stripped ROS membranes and purified PDE. The PDE activation observed with the ADP-ribosylated transducin was only slightly reduced from that observed with the control. Because the incubation without R* lasted only 6 h, the sample lacking NAD^+ would be expected to bind about 11% more nucleotide than would the NAD^+-containing

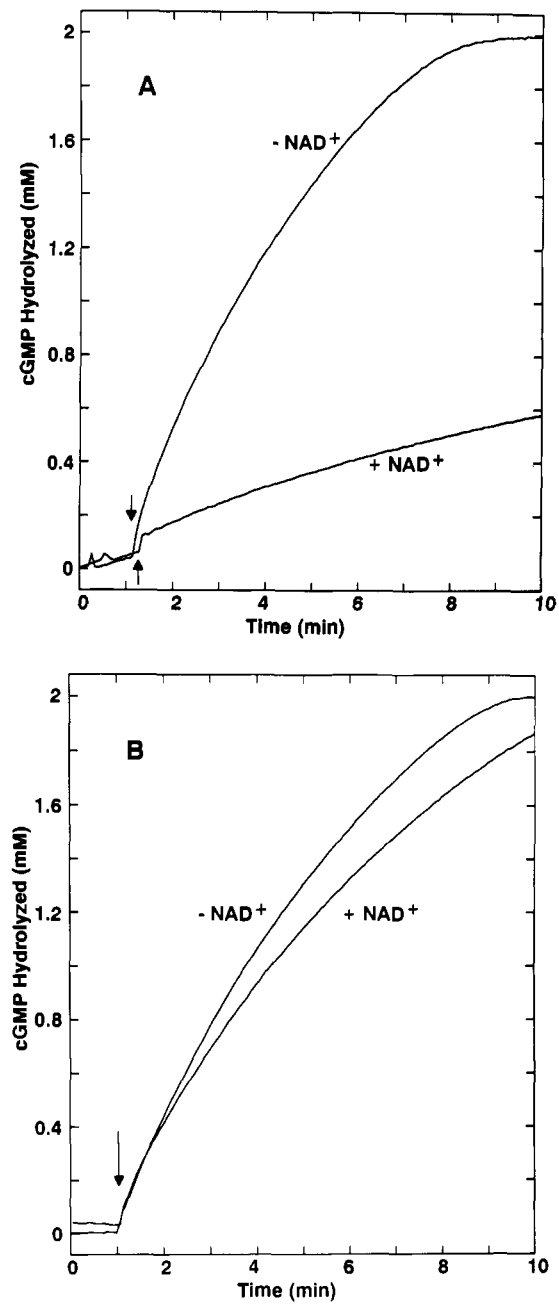

FIGURE 4: PDE activation in PTX-treated ROS stimulated by (A) GTP or by (B) Al^{3+} and F^-. ROS membranes were treated with PTX in the presence or absence of NAD^+, and PDE activity was assayed using the pH recording method (2.8 μM R*). (A) cGMP (2 mM) was present initially, and at the time indicated by the arrow, GTP (50 μM) was added. (B) PTX-treated ROS were incubated for 10 min with 4 mM NaF and 0.03 mM $AlK(SO_4)_2$, and cGMP (2 mM) was added at the indicated times.

sample after R* was added. The activation required the presence of GTPγS, and the gel-filtered transducin samples were carefully checked for PDE activity to confirm that the apparent activation was not due to PDE contamination. Such contamination is usually present at high levels (0.03–0.1% of total protein) in transducin preparations that have been through only one column purification step and at very high levels in GTP extracts of hypotonically washed ROS (Wensel & Stryer, 1986; L. Ramdas and T. Wensel, unpublished observations).

Discussion

Nucleotide Exchange. The spontaneous nucleotide exchange reported here occurs on a time scale of hours, and is

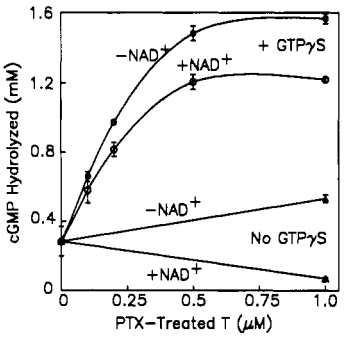

FIGURE 5: PDE activation in reconstituted membranes. Purified transducin was treated with PTX in the presence or absence of NAD^+ and was tested for ADP-ribosylation by mobility shift (results are shown in the top panel of Figure 1). Both samples were incubated with GTPγS (200 μM) for 6 h at 37 °C to allow spontaneous nucleotide exchange. They were added to urea-stripped ROS containing purified PDE at a ratio of 74 R*/PDE, and the reconstituted membranes were assayed for PDE activity by measuring the hydrolysis of [^{3}H]cGMP during a 10-min incubation (4 nM PDE). Control samples (No GTPγS) were subjected to identical treatment except that no GTPγS was added.

slower than the kinetics observed with other G proteins in the absence of activated receptors. For example, G_o (Higashijima et al., 1987) released GDP with rate constants ranging from 10^{-3} s^{-1} at <1 nM Mg^{2+} to 2×10^{-3} s^{-1} at 2 mM Mg^{2+} (the concentration used in the studies reported here). G_s (Northup et al., 1982) bound GTPγS with rate constants of (6.4–8.9) $\times 10^{-4}$ s^{-1} over the range of 10–100 μM GTPγS (10 mM Mg^{2+}). G_i bound 20 μM GTPγS with a rate constant of $\sim 10^{-3}$ s^{-1} (20 mM Mg^{2+}; Bokoch et al., 1984) and released GDP with a rate constant of 4.7×10^{-4} s^{-1} (no Mg^{2+}; Ferguson et al., 1986). Comparison of transducin's observed rate constant of (1–2) $\times 10^{-4}$ s^{-1} to the value of 10^3 s^{-1} observed for R*-catalyzed GTP exchange with saturating levels of GTP (Vuong et al., 1984) indicates a rate enhancement of (5–10) $\times 10^6$ for GDP release. Thus, transducin activation appears to be more tightly coupled to photoexcited rhodopsin than the activation of other G proteins is coupled to agonist-occupied receptors. However, our finding that GDP release appears to be rate-limiting is in agreement with results obtained for other G proteins.

Our finding that spontaneous nucleotide exchange rates are limited by GDP release at 10 μM GTPγS is consistent with the second-order rate constant of 10^7 M^{-1} s^{-1} reported previously for transducin (Wessling-Resnick & Johnson, 1987). A second-order rate constant of this magnitude implies that at GTPγS concentrations much greater than 20 pM, the slow [(1–2) $\times 10^{-4}$ s^{-1}] first-order process of GDP release should be rate-limiting, consistent with our results. Results were presented (Figures 1 and 2; Wessling-Resnick & Johnson, 1987) at 0.5 μM GTPγS that were consistent with an apparent first-order rate constant of $\sim 10^{-4}$ s^{-1}. However, these authors reported a nearly linear dependence of the initial rate of exchange on GTPγS concentration up to 1 μM, where initial velocities of $\sim 40 \times 10^{-4}$ s^{-1} [transducin]$^{-1}$ were observed at room temperature (Figure 3; Wessling-Resnick & Johnson, 1987). This rate is more than 20-fold higher than the rate we observe with a 10-fold higher GTPγS concentration (10 μM) at a higher temperature (37 °C). It was recently reported that rapid nucleotide exchange by transducin in the absence of R* can be explained by R* contamination of transducin prepared by common procedures (Fawzi & Northup, 1990). When R* was rigorously excluded, at 30 °C rate constants in the range of (0.17–0.3) $\times 10^{-4}$ s^{-1} were observed, somewhat slower than our values of (1–2) $\times 10^{-4}$ s^{-1} obtained at 37 °C. Because ADP-ribosylation, which blocks catalysis by R*, has little effect on our kinetic results, it is unlikely that the exchange kinetics reported here are enhanced by R* remaining in the transducin sample after chromatography. The discrepancy can be explained partly by the difference in temperatures. We have found that nucleotide exchange at 23 °C is approximately 3-fold slower than at 37 °C (L. Ramdas and T. Wensel, unpublished results), so the rate constant at 30 °C is expected to be about 1.7-fold lower. However, the discrepancy is primarily due to the fact that our data have been normalized to the maximal level of binding in a 20–24-h incubation, rather than to the total transducin present. This procedure accounts for any inactive (i.e., incapable of binding nucleotide) protein, but is only possible if the exchange reaction is followed over very long times. With a rate constant of 10^{-4} s^{-1}, after 60 min only 30% of the maximal nucleotide exchange would have taken place, but even for the slowest reported rate constant of 0.17×10^{-4} s^{-1}, the amount of bound nucleotide after a 24-h incubation should deviate from the equilibrium value by no more than 23%. Multiplying the first-order rate constant of 0.97×10^{-4} s^{-1}, obtained at 10 μM GTPγS (Figure 2A), by the fraction of transducin that had nucleotide bound after 24 h at 37 °C (0.33) gives a rate constant of 0.3×10^{-4} [transducin]$^{-1}$ s^{-1}, consistent with the initial velocity results of Fawzi and Northup (1990) obtained at 30 °C. The loss of total nucleotide binding activity (~40%) that we observed during the prolonged incubation can also lead to overestimation of the exchange rate constant. If the loss of binding activity is assumed to follow first-order kinetics, with an inactivation rate constant two-thirds the magnitude of the nucleotide exchange rate constant (this ratio would produce the observed stoichiometry after 20 h), then the true nucleotide exchange rate constant could actually be equal to only 0.6 times the value we have calculated.

The heterogeneity of nucleotide binding sites deserves further study. While it may to some extent reflect the partial denaturation observed during long incubations at 37 °C, evidence for more than one type of binding site has been observed in previous studies of rapid R*-catalyzed nucleotide exchange (Bennett & Dupont, 1985; Yamanaka et al., 1985, Figure 4A; Sitaramayya et al., 1988; Kohnken & McConnell, 1985). Because the concentration of GTP is relatively high in ROS (~2 mM in frog ROS; Robinson & Hagins, 1979), and because low-affinity binding has been reported to be associated with a fast GTPase rate (Sitaramayya et al., 1988), this low-affinity binding may be significant for transducin function. The low-affinity binding may not be directly involved in triggering the activation of T_α, because it has been observed only in binding and GTPase experiments, and not in studies of the dependence of PDE activation on nucleotide concentration. While the different sites can be distinguished by their very different affinities, they are not easily distinguished by the kinetics of binding in the absence of R*. All the nucleotide exchange kinetic data we have obtained, at nucleotide concentrations from 3 to 50 μM, and regardless of whether GTP uptake, GTPγS uptake, or GDP release was monitored, can be fit to single-exponential curves with rate constants in the range (0.9–2) $\times 10^4$ s^{-1}. The weak [GTPγS] dependence of the exchange rate constant observed at high [GTPγS] (Figure 2C inset) may reflect faster exchange at a low-affinity site.

Comparison to Previous Studies of PTX Effects. In a study of the effects of PTX on transducin (Rybin et al., 1989), it was reported that ADP-ribosylated transducin was incapable of exchanging bound GDP for GppNHp, and consequently could not hydrolyze GTP or activate PDE. However, these

experiments were carried out for short times (<100 min), and the nucleotide exchange activity of PTX-inactivated transducin was compared to that of a preparation that hydrolyzed GTP at a rate of 1.5×10^{-3} s^{-1} [transducin]$^{-1}$. The latter rate is approximately 10 times too fast to be accounted for by transducin alone, and may be due to trace contamination with R* in the nonchromatographed GTP extracts that were used.

Sunyer et al. (1989) examined the effects of ADP-ribosylation on G_i and found, in agreement with our results for transducin, that PTX treatment of G_i did not block its ability to hydrolyze GTP and release GDP, to bind GppNHp, or to inhibit adenylate cyclase when bound to GppNHp. The suggestion (Sunyer et al., 1989) that PTX blocks the ability of GTP, but not of nonhydrolyzable analogues, to induce the activated "G*" state that regulates effector function cannot be readily tested for transducin. The reason is that the steady-state level of T_α–GTP in the absence of R* catalysis of exchange is given by $[T_\alpha\text{–GTP}]/[T_\alpha\text{–GDP}]$ = (rate constant for GDP release)/(rate constant for hydrolysis of bound GTP). This ratio under our conditions is $(1\text{–}2) \times 10^{-4}$ $s^{-1}/[(1.6\text{–}4) \times 10^{-2}$ $s^{-1}] = (2.5\text{–}12.5) \times 10^{-3}$. Such a small fraction of GTP-bound transducin is not easily detectable either by fluorescence or by PDE activation even if it is all in the activated conformation. However, the differences between GTP and GTPγS effects on transducin can readily by explained by the difference in steady-state levels of GTPγS and GTP bound to transducin without invoking a fundamental difference in the conformations induced by GTP and nonhydrolyzable analogues in the absence of R*. The GTPase rates reported for G_i in the absence of receptors (Sunyer et al., 1984, 1989) were $(1.67\text{–}1.77) \times 10^{-4}$ s^{-1} $[G_i]^{-1}$, values similar to the GDP release rates we observe for transducin in the absence of R*. The failure of GTP to separate the βγ subunits from ADP-ribosylated α subunits of G_i and G_o (Huff & Neer, 1986), despite the ability of GTPγS to do so, can also be explained by GTP hydrolysis if the effects of PTX on G_i and G_o are similar to its effects on transducin.

Our results do not allow a definite conclusion about interactions between the PTX site and the site of $T_{\beta\gamma}$ binding. It has been shown (Huff & Neer, 1986) that ADP-ribosylation of $G_{o\alpha}$ by PTX does not interfere either with binding of βγ subunits to G_α subunits or with release of βγ upon binding GTPγS. However, $T_{\beta\gamma}$ greatly enhances the PTX-catalyzed reaction (West et al., 1985), and the βγ complex has been shown to participate in transducin binding to R* (Fung, 1983).

Implications for Transducin Structure and Function. A number of models have been proposed for spatial and functional relationships among regions of the primary sequence of T_α and other G proteins (Hingorani & Ho, 1987; Deretic & Hamm, 1987; Bourne et al., 1988; Holbrooke & Kim, 1989). Results of the kind described here, defining functional sites which do or do not interact strongly, can help to provide constraints for the construction of structural models, and for correlating function with three-dimensional structural information when it becomes available.

The R* binding site of transducin is clearly coupled in a very strong way to the nucleotide binding site, as revealed by R*'s dramatic enhancement of nucleotide exchange kinetics. However, as demonstrated here, it is possible to disrupt one site (by ADP-ribosylation) without measurably affecting the other. Likewise, those regions of the α subunit that are involved in the conformational change essential for PDE interactions, as well as those directly involved in nucleotide binding, appear to be distinct from, and not tightly coupled to, the C-terminal region of T_α where R* appears to bind and where ADP-ribosylation occurs. These results would seem to rule out, at least for the case of transducin, the possibility that pertussis toxin "locks" G proteins in the GDP form (Rybin et al., 1989), and support the idea that ADP-ribosylation merely blocks R* binding (Van Dop et al., 1984).

Results from PTX effects complement and confirm those obtained from proteolytic digestion and analysis of mutant G proteins. Removal of the carboxyl-terminal 5000-Da fragment from GppNHp-activated T_α (Hurley et al., 1984) does not eliminate its ability to activate PDE (Fung & Nash, 1983), and removal of the carboxyl terminal of $G_{o\alpha}$ with carboxypeptidase A does not prevent binding to βγ (Neer et al., 1988). On the other hand, removal of the amino-terminal 1000 Da of T_α does abolish βγ interactions (Navon & Fung, 1987). The *unc* mutation, a single amino acid substitution near the carboxyl terminal of $G_{s\alpha}$ (Sullivan et al., 1987), blocks receptor interactions. Chimeric G_α constructs have shown that residues critical for both receptor and effector interactions lie in the carboxyl terminal 40% of the α chains (Masters et al., 1988) but that the last 38 residues of α_s can be replaced with the corresponding 36 residues from α_i without loss of the ability to activate adenylyl cyclase (Osawa et al., 1990). All these results confirm that the cysteine residue ADP-ribosylated by PTX is in a region of G protein α subunits that is critical for receptor (or R*) interactions but is not involved directly in effector, nucleotide, or βγ interactions, and does not interact strongly with the "switch" domain (Holbrook & Kim, 1989) that has been proposed to be essential for triggering the activated conformation.

Because many functional properties are retained by ADP-ribosylated transducin, the pertussis toxin catalyzed reaction is useful for studying the high-affinity form of transducin that remains tightly membrane-bound in the GTP state, and is much more potent in PDE stimulation that GTP-solubilized transducin (Wensel & Stryer, 1988). We have found (L. Ramdas, R. M. Disher, and T. G. Wensel, unpublished observations) that this form of transducin can be ADP-ribosylated by PTX in membranes that have been extensively washed with GTP and that radiolabeling with [^{32}P]NAD^+ facilitates monitoring the detergent solubilization of this protein.

The results presented here also suggest that the ADP-ribosyl groups should be able to serve as nonperturbing probe sites for studying interactions with PDE. The ADP-ribosylation reaction represents a convenient approach to introducing spectroscopic reporter groups into a specific site. A fluorescent NAD^+ derivative can be used to incorporate a fluorescent ADP-ribose analogue into T_α using PTX (Hingorani & Ho, 1988). Because PDE subunits can be labeled with chromophoric sulfhydryl reagents without loss of activity (Wensel & Stryer, 1990), resonance energy transfer may provide a method for direct observation of interactions between transducin and PDE subunits.

Acknowledgments

We thank Dr. Justine Malinski for helpful comments on the manuscript.

Registry No. cGMP PDE, 9068-52-4; GTPγS, 37589-80-3; GDP, 146-91-8.

References

Bennett, N., & Dupont, Y. (1985) *J. Biol. Chem. 260*, 4156–4168.

Bigay, J., Deterre, P., Pfister, C., & Chabre, M. (1985) *FEBS Lett. 191*, 181–185.

Bigay, J., Deterre, P., Pfister, C., & Chabre, M. (1987) *EMBO J. 6*, 2907–2913.
Birnbaumer, L. (1990) *Annu. Rev. Pharmacol. Toxicol. 30*, 675–705.
Bokoch, G. M., Katada, T., Northup, J. K., Hewlett, E. L., & Gilman, A. G. (1983) *J. Biol. Chem. 258*, 2072–2075.
Bokoch, G. M., Katada, T., Northup, J. K., Ui, M., & Gilman, A. G. (1984) *J. Biol. Chem. 259*, 3560–3567.
Bourne, H. R., Masters, S. B., Miller, R. T., Sullivan, K. A., & Heideman, W. (1988) *Cold Spring Harbor Symp. Quant. Biol. 53*, 221–228.
Bradford, M. M. (1976) *Anal. Biochem. 72*, 248–254.
Codina, J., Hildebrandt, J. D., Iyengar, R., Birnbaumer, L., Sekura, R. D., & Manclark, C. R. (1983) *Proc. Natl. Acad. Sci. U.S.A. 80*, 4276–4280.
Deretic, D., & Hamm, H. E. (1987) *J. Biol. Chem. 262*, 10839–10847.
Fawzi, A. B., & Northup, J. K. (1990) *Biochemistry 29*, 3804–3812.
Ferguson, K. M., Higashijima, T. H., Smigel, M. D., & Gilman, A. G. (1986) *J. Biol. Chem. 261*, 7393–7399.
Fong, H. K. W., Yoshimoto, K. K., Eversole-Cire, P., & Simon, M. I. (1988) *Proc. Natl. Acad. Sci. U.S.A. 85*, 3066–3070.
Fung, B. K.-K. (1983) *J. Biol. Chem. 258*, 10495–10502.
Fung, B. K.-K., & Nash, C. R. (1983) *J. Biol. Chem. 258*, 10503–10510.
Fung, B. K.-K., & Stryer, L. (1980) *Proc. Natl. Acad. Sci. U.S.A. 77*, 2500–2504.
Fung, B. K.-K., Hurley, J. B., & Stryer, L. (1981) *Proc. Natl. Acad. Sci. U.S.A. 78*, 152–156.
Gilman, A. G. (1987) *Annu. Rev. Biochem. 56*, 615–650.
Higashijima, T., Ferguson, K. M., Sternweis, P. C., Smigel, M. D., & Gilman, A. G. (1987) *J. Biol. Chem. 262*, 762–766.
Hildebrandt, J. D., Sekura, R. D., Codina, J., Iyengar, R., Manclark, C. R., & Birnbaumer, L. (1983) *Nature 302*, 706–709.
Hingorani, V. N., & Ho, Y.-K. (1987) *FEBS Lett. 220*, 15–22.
Hingorani, V. N., & Ho, Y.-K. (1988) *J. Biol. Chem. 263*, 19804–19808.
Holbrook, S. R., & Kim, S.-H. (1989) *Proc. Natl. Acad. Sci. U.S.A. 86*, 1751–1755.
Huff, R. M., & Neer, E. J. (1986) *J. Biol. Chem. 261*, 1105–1110.
Hurley, J. B., & Stryer, L. (1982) *J. Biol. Chem. 257*, 11094–11099.
Hurley, J. B., Simon, M. I., Teplow, D. B., Robishaw, J. D., & Gilman, A. G. (1984) *Science 226*, 860–862.
Kanaho, Y., Moss, J., & Vaughn, M. (1985) *J. Biol. Chem. 260*, 11493–11497. Katada, T., & Ui, M. (1982) *J. Biol. Chem. 257*, 7210–7216.
Kelleher, D. J., Dudycz, L. W., Wright, G. E., & Johnson, G. L. (1986) *Mol. Pharmacol. 30*, 603–608.
Kohnken, R. E., & McConnell, D. G. (1985) *Biochemistry 24*, 3803–3809.
Laemmli, U. K. (1970) *Nature (London) 227*, 680–685.
Liebman, P. A., & Evanczuk, T. (1982) *Methods Enzymol. 81*, 532–542.
Masters, S. B., Martin, M. W., Harden, T. K., & Brown, J. H. (1985) *Biochem. J. 227*, 933–937.
Masters, S. B., Sullivan, K. A., Miller, R. T., Beiderman, B., Lopen, N. G., Ramachandran, J., & Bourne, H. R. (1988) *Science 241*, 448–451.
Navon, S. E., & Fung, B. K.-K. (1987) *J. Biol. Chem. 262*, 15746–15751.
Neer, E. J., Pulsifer, L., & Wolf, L. G. (1988) *J. Biol. Chem. 263*, 8996–9000.
Northup, J. K., Smigel, M. D., & Gilman, A. G. (1982) *J. Biol. Chem. 257*, 11416–11423.
Osawa, S., Dhanasekaran, N., Woon, C. W., & Johnson, G. L. (1990) *Cell 63*, 697–706.
Phillips, W. J., & Cerione, R. A. (1988) *J. Biol. Chem. 263*, 15498–15505.
Ribeiro-Neto, F. A. P., & Rodbell, M. (1989) *Proc. Natl. Acad. Sci. U.S.A. 86*, 2577–2581.
Robinson, W. E., & Hagins, W. A. (1979) *Nature (London) 280*, 398–408.
Rybin, V. O., Gureeva, A. A., & Tkachuk, V. A. (1989) *Membr. Biochem. 8*, 115–126.
Shinozawa, T., Uchida, S., Martin, E., Cafiso, D., Hubbell, W., & Bitensky, M. (1980) *Proc. Natl. Acad. Sci. U.S.A. 77*, 1408–1411.
Sitaramayya, A., Casadevall, C., Bennett, N., & Hakki, S. (1988) *Biochemistry 27*, 4880–4887.
Sternweis, P. C., & Robishaw, J. D. (1984) *J. Biol. Chem. 259*, 13806–13813.
Strathmann, M., & Simon, M. I. (1990) *Proc. Natl. Acad. Sci. U.S.A. 87*, 9113–9117.
Stryer, L., & Bourne, H. R. (1986) *Annu. Rev. Cell Biol. 2*, 391–419.
Sullivan, K. A., Miller, R. T., Masters, S. B., Beiderman, B., Heideman, W., & Bourne, H. R. (1987) *Nature 330*, 758–760.
Sunyer, T., Codina, J., & Birnbaumer, L. (1984) *J. Biol. Chem. 259*, 15447–15451.
Sunyer, T., Monastirsky, B., Codina, J., & Birnbaumer, L. (1989) *Mol. Endocrinol. 3*, 1115–1124.
Thompson, W. J., & Appleman, M. M. (1971) *Biochemistry 10*, 311–316.
Van Dop, C., Yamanaka, G., Steinberg, F., Sekura, R. D., Manclark, C. R., Stryer, L., & Bourne, H. R. (1984) *J. Biol. Chem. 259*, 23–26.
Vuong, T. M., Chabre, M., & Stryer, L. (1984) *Nature 311*, 659–661.
Watkins, P. A., Moss, J., Burns, D. L., Hewlett, E. L., & Vaughan, M. (1984) *J. Biol. Chem. 259*, 1378–1381.
Watkins, P. A., Burns, D. L., Kanaho, Y., Liu, T.-Y., Hewlett, E. L., & Moss, J. (1985) *J. Biol. Chem. 260*, 13478–13482.
Wensel, T. G., & Stryer, L. (1986) *Proteins: Struct., Funct., Genet. 1*, 90–99.
Wensel, T. G., & Stryer, L. (1988) in *Enzyme Dynamics and Regulation* (Chock, P. B., Huang, C. Y., Tsou, C. L., & Wang, J. H., Eds.) pp 102–112 Springer-Verlag, New York.
Wensel, T. G., & Stryer, L. (1990) *Biochemistry 29*, 2155–2161.
Wessling-Resnick, M., & Johnson, G. L. (1987) *Biochemistry 26*, 4316–4323.
West, R. E., Jr., Moss, J., Vaughan, M., Liu, T., & Liu, T.-Y. (1985) *J. Biol. Chem. 260*, 14428–14430.
Yamanaka, G., Eckstein, F., & Stryer, L. (1985) *Biochemistry 24*, 8094–8101.